# EFFECT OF THERMAL CONDUCTIVITY ON THE INITIATION, GROWTH AND BANDWIDTH OF ADIABATIC SHEAR BANDS

## R. C. BATRA and C. H. KIM

Department of Mechanical and Aerospace Engineering and Engineering Mechanics, University of
Missouri–Rolla, Rolla, MO 65401-0249, U.S.A.

**Abstract**—We ascertain the effect of thermal conductivity on the initiation and growth of shear bands in a structural steel by analyzing the development of shear bands in a block undergoing overall adiabatic simple shearing deformations. The material of the block is assumed to exhibit strain and strain-rate hardening, and thermal softening. Three constitutive relations, namely, the Litonski law, the Bodner–Partom law, and the Johnson–Cook law, have been used to model the thermoviscoplastic response of the material. For each material model, five values of thermal conductivity differing by three orders of magnitude have been used.

It is found that an increase in the value of the thermal conductivity delays the initiation and slows down the subsequent development of the shear band. For the Litonski law and Johnson–Cook law, the band width tends to zero as the thermal conductivity approaches zero. However, for the Bodner–Partom law, the band width is non-zero even when the thermal conductivity is set equal to zero.

## 1. INTRODUCTION

Adiabatic shear banding refers to the localization phenomenon that occurs during high strain-rate plastic deformation, such as machining, shock impact loading, ballistic penetration, and metal forming processes. As shear bands precede material fracture, the discernment of variables that enhance or retard their initiation and growth will make possible design of materials and manufacturing techniques that are less conducive to the formation of shear bands. Variables that are believed to have a noticeable effect on the development of shear bands include material strain-rate sensitivity, thermal diffusivity, thermal softening, strain hardening, inertia forces, and the initial temperature of the specimen. Here we explore in some detail the effect of the thermal conductivity or the thermal length on the initiation and subsequent growth of shear bands in a viscoplastic block undergoing overall adiabatic simple shearing deformations at an average strain-rate of $3300 \, s^{-1}$. The values of material parameters, except for the thermal conductivity, are those for a typical structural steel. Five values of the thermal conductivity, namely, 0, 5, 50, 500, and $5000 \, W/m \, °C$, have been used to assess its effect on the development of shear bands.

In studying the growth of shear bands in the center of a finite slab after initiation at a small imperfection, Merzer [1] concluded that the final width of the band depends on the thermal diffusivity and the overall strain rate. Wu and Freund [2], in studying the formation of shear bands at a moving boundary, concluded that thermal diffusivity has little influence on the final shape of the band. The detailed geometry and constitutive equations considered in these two papers are different. In both papers, there are two natural length scales, one arising from the rate effect in the constitutive equation, and the other from heat conductivity. In the latter paper, these two scales have been arbitrarily set equal to each other, and in the former paper the relative effect of heat conductivity has been examined parametrically for the Bodner–Partom constitutive relation. Wu and Freund [2] also showed that for linear strain-rate sensitivity the shear layer thickness increased with boundary velocity, but the reverse happened for logarithmic rate sensitive materials. Possible reasons for opposing effects of thermal conductivity reported in these two papers could be (a) different problems studied, and/or (b) different constitutive relations employed. Here we use three constitutive relations, namely, the Litonski law, the Bodner–Partom law, and the Johnson–Cook law, to model the viscoplastic response of the material. It is found that for all three constitutive relations, the computed band width increases with increase in the value of the thermal conductivity, suggesting thereby that

the apparently contradictory results reported in the above-cited two papers are due to the different phenomenon presumed for the occurrence of adiabatic shear bands.

In recent years there have been numerous experimental [3–7], analytical [8–15], and numerical [16–23] investigations aimed at increasing our understanding of the localization of the deformation into shear bands. Shawki and Clifton [24] have reviewed much of the literature dealing with the one-dimensional shear banding problem. Recently, there have been a few studies [25–35] of the phenomenon of shear banding in plane strain deformations of a thermally softening viscoplastic block. Anand et al. [12] have extended the one-dimensional perturbation analysis of Clifton and coworkers [36] to three-dimensional problems. They also included the effect of hydrostatic pressure on plastic flow, so as to better model the behavior of polymeric materials. Their analysis predicts that for pressure-sensitive materials, shear bands can initiate in two directions even in simple shear.

## 2. FORMULATION OF THE PROBLEM

In terms of non-dimensional variables, equations governing the dynamic thermomechanical deformations of a viscoplastic block undergoing overall adiabatic simple shearing deformations are

$$\alpha w \dot{v} = (ws)_{,y}, \qquad 0 < y < 1, \tag{2.1}$$

$$w\dot{\theta} = \beta(w\theta_{,y})_{,y} + ws\dot{\gamma}_p, \qquad 0 < y < 1, \tag{2.2}$$

$$\dot{s} = \mu(v_{,y} - \dot{\gamma}_p), \tag{2.3}$$

$$\dot{\gamma}_p = g(s, \gamma_p, \theta). \tag{2.4}$$

Here $v$, $\theta$, $s$, $\gamma_p$ and $w$ represent, respectively, the velocity of a particle in the direction of shearing taken to be along the $x$-axis, temperature rise, shear stress, plastic strain, and thickness of the block. Furthermore, $\beta$ is the thermal diffusivity, $\mu$ is the shear modulus, $\alpha$ signifies the effect of inertia forces relative to the flow stress of the material, a superimposed dot indicates material time derivative, and a comma followed by $y$ implies partial differentiation with respect to $y$. Equation (2.1) expresses the balance of linear momentum, equation (2.2) the balance of internal energy, equation (2.3) Hooke's law written in the rate form, and equation (2.4) is a constitutive relation for $\dot{\gamma}_p$. The viscoplastic flow rules differ in the functional forms of $g$. Fourier's law of heat conduction has been used in equation (2.2). Also, we have assumed that the shear strain-rate has additive decomposition into elastic and plastic parts, and all of the plastic working, given by the second term on the right-hand side of equation (2.2), is converted into heat. We note that Sulijoadikusumo and Dillon [37] and Farren and Taylor [38] found that only 90–95% of the plastic work done is responsible for raising the temperature of the body.

The dimensional variables, indicated below by a superimposed bar, are related to the non-dimensional variables as follows:

$$\bar{y} = yH, \qquad \bar{w} = wH, \qquad \bar{t} = tH/v_0, \qquad \bar{\theta} = \theta\theta_0, \qquad \theta_0 = \sigma_0/\rho c,$$

$$\bar{s} = s\sigma_0, \qquad \alpha = \rho v_0^2/\sigma_0, \qquad \bar{\mu} = \mu\sigma_0, \qquad \beta = k/(\rho c v_0 H),$$

$$\dot{\bar{\gamma}}_p = \dot{\gamma}_p v_0/H. \tag{2.5}$$

In equation (2.5), $H$ is the height of the block, $v_0$ is the final value of the speed imposed on the top surface of the block, $\rho$ is the mass density, $t$ is the time elapsed, $\sigma_0$ is the yield stress in a quasistatic simple shear test, $k$ is the thermal conductivity, and $c$ is the specific heat. Hereafter, we drop the superimposed bars and indicate a dimensional quantity by specifying its units.

For the initial and boundary conditions we take

$$\theta(y, 0) = 0, \qquad v(y, 0) = 0, \qquad s(y, 0) = 0, \qquad \gamma_p(y, 0) = 0,$$

$$\theta_{,y}(0, t) = 0, \qquad \theta_{,y}(1, t) = 0, \qquad v(0, t) = 0,$$

$$v(1, t) = t/0.01, \qquad 0 \le t \le 0.01,$$

$$= 1, \qquad t \ge 0.01. \tag{2.6}$$

That is, the block is initially stress free, is undeformed, is at rest, and has a uniform temperature, normalized to be zero. The overall deformations of the block are taken to be adiabatic and the lower surface is at rest, whereas the upper surface is assigned a velocity that increases from 0 to 1 in a non-dimensional time of 0.01 and then stays equal to 1.0. The block is taken to be thinnest at the center, $y = \frac{1}{2}$, and thickest at the boundary surfaces, $y = 0$, 1, with the thickness variation given by

$$w(y) = w_0\left[1 + \frac{\delta}{2}\sin\left(\frac{1}{2} + 2y\right)\pi\right].$$

$\qquad(2.7)$

We note that Marchand and Duffy [7] reported nearly 10% variation in the thickness of the steel tubes they tested in torsion. Our choice of locating the thinnest section at the center is for convenience only and should not affect the computed results.

## 3. VISCOPLASTIC FLOW RULES

### 3.1 Litonski's law

Wright and Batra [18] modified the Litonski law to account for elastic unloading of a material point. They postulated that

$$\dot{\gamma}_p = \Lambda s,$$

$\qquad(3.1)$

$$\Lambda = \max\left[0, \left(\left(\frac{s}{(1 - v\theta)\left(1 + \frac{\psi}{\psi_0}\right)^n}\right)^{1/m} - 1\right)\bigg/bs\right],$$

$\qquad(3.2)$

$$\dot{\psi} = s\dot{\gamma}_p/(1 + \psi/\psi_0)^n.$$

$\qquad(3.3)$

We may view $\psi$ as an internal variable that describes the work hardening of the material. Its evolution equation (3.3) implies that the rate of growth of $\psi$ is proportional to the plastic working. In equation (3.2), $(1 - v\theta)$ describes the softening of the material as a result of its heating, $b$ and $m$ characterize its strain-rate sensitivity, and $\psi_0$ and $n$ its work hardening. Equations (3.1) and (3.2) imply that

$$\dot{\gamma}_p = 0 \quad \text{if} \quad s \leq (1 - v\theta)(1 + \psi/\psi_0)^n.$$

$\qquad(3.4)$

Thus $s = (1 - v\theta)(1 + \psi/\psi_0)^n$ describes a loading surface, and if the local state given by $(s, \psi, \theta)$ lies inside or on this surface, the plastic strain-rate is zero and the material then is deforming elastically. Besides $\sigma_0$, which has been used to non-dimensionalize stress-like quantities, five material parameters, $v$, $b$, $m$, $\psi_0$, and $n$ are needed to specify the viscoplastic response of the material.

### 3.2 Bodner–Partom law

Bodner and Partom [39] assumed that there is no loading surface and that plastic strain-rate $\dot{\gamma}_p$, albeit very small at low values of $s$, is always non-zero. Their constitutive relation can be written as

$$\dot{\gamma}_p = D_0 \exp\left[-\frac{1}{2}\left(\frac{z^2}{3s^2}\right)^n\right], \qquad n = \frac{a}{T} + b,$$

$\qquad(3.5)$

$$z = z_1 - (z_1 - z_0)\exp(-mW_p),$$

$\qquad(3.6)$

$$\dot{W}_p = s\dot{\gamma}_p.$$

$\qquad(3.7)$

Here $T$ is the absolute temperature of a material particle, $W_p$ is the plastic work done, $z$ may be regarded as an internal variable, and $D_0$ is the limiting value of the plastic strain-rate, usually taken as $10^8\,\text{s}^{-1}$. Besides $D_0$, we need to specify $a$, $z_1$, $z_0$, $m$, and $b$ to characterize the material.

### 3.3 Johnson–Cook law

Johnson and Cook [40] tested 12 materials in simple shear and compression at different strain-rates and found that

$$\dot{\gamma}_p = \exp\left[\left(\frac{s}{(A + B\gamma_p^n)(1 - \bar{T}^v)} - 1.0\right)\Big/C\right], \tag{3.8}$$

$$\bar{T} = (\theta - \theta_0)/(\theta_m - \theta_0), \tag{3.9}$$

describe well the test data. For $\theta_m$ equal to the melting temperature of the material and $\theta_0$ equal to the ambient temperature, they tabulated values of $A$, $B$, $n$, $v$, and $C$ for 12 materials. It should be noted that there is no loading surface assumed in this case, too.

## 4. RESULTS

### 4.1 Computational considerations

The governing equations (2.1)–(2.4) with the function $g$ given by one of the flow rules described in the previous section are highly nonlinear, and are difficult to solve analytically under the side conditions (2.5) and (2.6). An approximate solution of these equations has been computed numerically by using the finite element method. The partial differential equations (2.1)–(2.4) are first reduced to a set of coupled nonlinear ordinary differential equations by using the Galerkin approximation. The stiff ordinary differential equations are integrated with respect to time by the Gear method [41]. For this purpose, the subroutine LSODE included in the package ODEPACK developed by Hindmarsh [42] is used. The subroutine adjusts the time increment adaptively until a solution of the stiff ordinary differential equations has been computed to the desired accuracy.

In the computation of results given below, the following values of various material parameters were used: $\rho = 7860 \text{ kg/m}^3$, $\sigma_0 = 405 \text{ MPa}$, and $c = 473 \text{ J/kg} °C$;

(a) Litonski's law: $v = 6 \times 10^{-4}/°K$, $\psi_0 = 0.012$, $m = 0.01872$, $n = 0.054$, and $b = 10^4 \text{ s}$;

(b) Bodner–Partom law: $D_0 = 1000$, $z_1 = 3.778$, $z_2 = 3.185$, $m = 2.5$, $a = 1800°K$, and $b = 0$;

(c) Johnson–Cook law: $A = 0.275$, $B = 1.433$, $C = 36$, $n = 0.054$, $v = 0.8$, $\theta_m = 1800°K$ and $\theta_0 = 300°K$.

The values of geometric parameters used are $H = 2.5 \text{ mm}$, $w_0 = 0.38 \text{ mm}$, and $\delta = 0.05$. The values of the material parameters given above are such that for $k = 50 \text{ W/m} °C$ and average strain-rate of $3300 \text{ s}^{-1}$, the average shear stress $s_a$ versus the average shear strain $\gamma_{avg}$ curve approximated well the experimental stress–strain curve for HY-100 steel given by Marchand and Duffy [7]. The average shear stress $s_a$ is defined as

$$s_a = \int_0^1 s(y, t)\, dy.$$

For $\dot{\gamma}_{avg} = 3300 \text{ s}^{-1}$, the inertia effects do not play a noticeable role, and the shear stress depends upon $y$ mainly because of the dependence of $w$ upon $y$. Subsequently, the values of material parameters and the average strain-rate were kept fixed, and results were computed for $k = 0$, 5, 50, 500, and 5000 W/m °C. These results are identified below as follows.

| Curve type | $k$ (W/m °C) |
|---|---|
| - - - - - | 0 |
| ———— | 5 |
| — — — | 50 |
| — — — — - | 500 |
| — — — — — — — | 5000 |

For the Litonski law, and for $k = 0$ and 5 W/m °C, results could not be computed satisfactorily once the shear stress began to drop precipitously.

## 4.2 Numerical results

Figure 1 depicts the average shear stress $s_a$ versus the average shear strain $\gamma_{avg}$ curves for the three constitutive models and the five values of the thermal conductivity $k$. For each constitutive relation used, the $s_a$–$\gamma_{avg}$ curves for $k = 0$ and 5 W/m °C are essentially identical with each other. The value of $\gamma_{avg}$ at which $s_a$ begins to drop increases a little with an increase in the value of the thermal conductivity. However, the rate of stress drop decreases dramatically as the value of $k$ is increased from 50 to 500 W/m °C as compared with that when $k$ is increased from 5 to 50 W/m °C. For each value of $k$ considered, the value of $\gamma_{avg}$ when the average shear stress $s_a$ becomes maximum is the least for the Johnson–Cook law. The $s_a$–$\gamma_{avg}$ curves look alike for the Litonski law and the Bodner–Partom law, except that the rate of stress drop is a little less for the Bodner–Partom law than for the Litonski law.

Figure 2 depicts the evolution of the homologous temperature, defined as the ratio of the absolute temperature of a material point to the melting temperature of the material, at the center of the specimen. Because of the non-dimensional variables being used herein, the horizontal scale representing the average strain can also be interpreted as the time elapsed. For each of the three constitutive relations used, the rate of temperature rise is largest for $k = 0$ and decreases as the value of $k$ is increased. For $k = 0$ and 5 W/m °C, the Johnson–Cook law gives the steepest rise in the temperature at the specimen center. It should be recalled that the shear stress is greatest at the specimen center because the thickness there is the least. For $k = 50$ W/m °C, the Litonski law gives the most rapid rate of temperature increase at the center of the specimen. The value of $\gamma_{avg}$ when the temperature at the specimen center begins to rise sharply is different for the three constitutive relations. For $k = 5000$ W/m °C and for
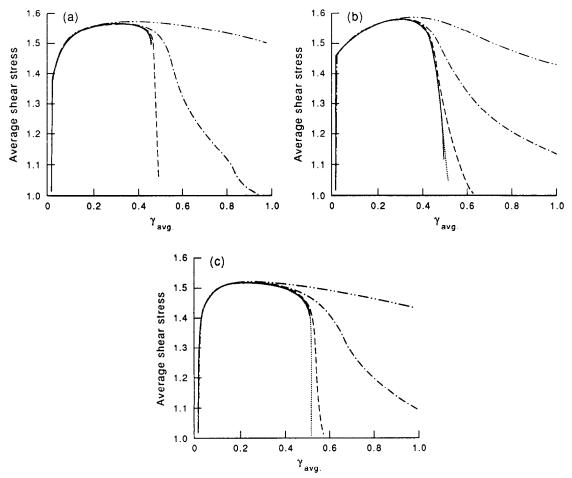


Fig. 1. Average shear stress vs average shear strain for the three constitutive relations and the five values of the thermal conductivity. (a) Litonski, (b) Bodner–Partom, (c) Johnson–Cook.
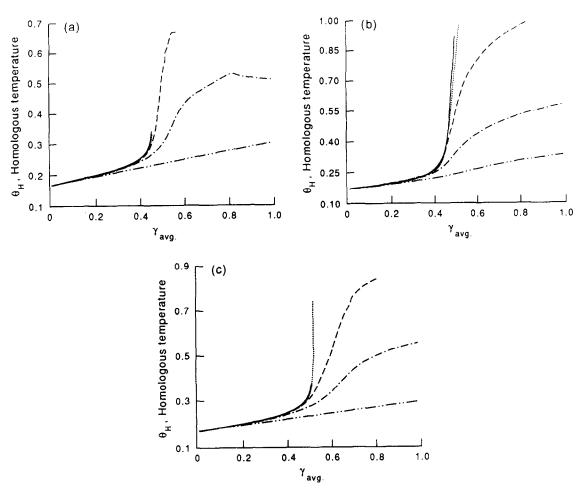
Fig. 2. Evolution of the homologous temperature at the center of the specimen for the three constitutive relations and five values of the thermal conductivity. (a) Litonski, (b) Bodner–Partom, (c) Johnson–Cook.

$0 < \gamma_{avg} < 1$, the temperature at the specimen center increases nearly linearly for each of the three constitutive relations used, except that for the Bodner–Partom law the slope of the $\theta_H$ vs. $\gamma_{avg}$ curve increases at $\gamma_{avg} \simeq 0.4$. As the value of $k$ increases, the heat conducted away from the central hotter region to the outer parts of the specimen increases and the rate of temperature rise at the specimen center decreases. Because of the adiabatic boundary conditions assumed, the temperature everywhere in the specimen increases.

As a significant part of the temperature rise occurs after the shear stress has attained its maximum value, we have plotted in Fig. 3 the homologous temperature $\theta_H$ at the specimen center versus $s_a/s_{max}$. For the Litonski law and the Johnson–Cook law, the $\theta_H$–$s_a/s_{max}$ curve corresponding to $k = 50$ W/m °C shows a second-order transition at $s_a/s_{max} \simeq 0.945$ and 0.92 respectively. For each of the three constitutive relations studied herein, the value of $\theta_H$, when $s_a/s_{max} = 1.0$, appears to be independent of $k$. This value of $\theta_H$ equals 0.2, 0.21, and 0.214 for the Johnson–Cook law, the Bodner–Partom law, and the Litonski law respectively. For the Bodner–Partom law, the $\theta_H$–$s_a/s_{max}$ curves for the five values of $k$ are essentially straight lines, and the slope of the straight line decreases with an increase in the value of $k$. It should be noted that for fixed values of $k$ and $s_a/s_{max}$, the temperature rise at the specimen center depends upon the constitutive relation employed. This is because the three constitutive relations give different rates of stress drop.

Figure 4 shows the shear strain at the specimen center, $\gamma_{loc}$, versus the average strain. The curves for the Bodner–Partom law differ from those for the Litonski law and the Johnson–Cook law. For the Bodner–Partom law, with an increase in the value of $k$, the slope of the
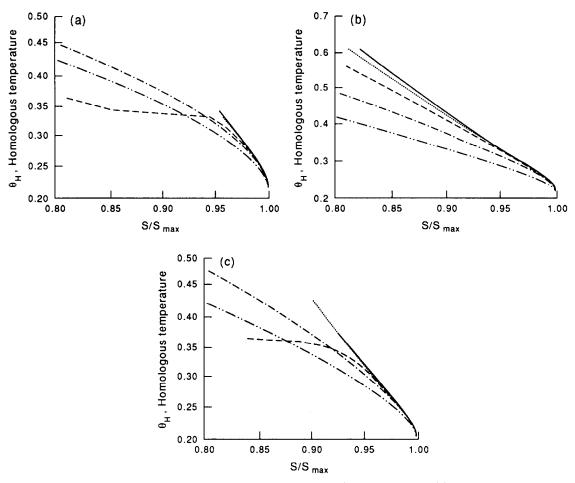
Fig. 3. Homologous temperature at the specimen center vs $s_a/s_{max}$. (a) Litonski, (b) Bodner–Partom, (c) Johnson–Cook.

$\gamma_{loc}-\gamma_{avg}$ curve when $s_a/s_{max} < 1$ decreases. For the Litonski law and the Johnson–Cook law, the $\gamma_{loc}-\gamma_{avg}$ curves for $k = 50$ W/m °C show similar qualitative behavior. However, $\gamma_{loc}$ increases more rapidly for the Litonski law than that for the other two constitutive relations. For $k = 5000$ W/m °C, $\gamma_{loc}$ increases very slowly, mainly because most of the heat developed near the specimen center due to plastic working is conducted away. For $k = 500$ W/m °C and the Litonski law, the local strain seems to have reached the saturation value at $\gamma_{avg} = 0.82$. A similar behavior was observed for the Johnson–Cook law at $\gamma_{avg} = 1.5$, but not for the Bodner–Partom law up to $\gamma_{avg} = 4.0$.

We recall that the thermal softening is described by essentially similar functions in the Litonski law and the Johnson–Cook law, but by a totally different functional relationship in the Bodner–Partom law. We believe that it is the difference in the thermal softening behavior stipulated in the three constitutive relations that accounts for the difference in the evolution of the temperature and hence the local strain at the specimen center.

A measure of the localization of the deformation at the specimen center is the ratio of the shear strain there to the average strain in the specimen. As localization of the deformation occurs in earnest when the shear stress has started to drop precipitously, we have plotted $\gamma_{loc}/\gamma_{avg}-s_a/s_{max}$ in Fig. 5. For the Bodner–Partom law, the curves for $k = 0$, 5, 50, and 500 W/m °C essentially coincide with each other, whereas that for $k = 5000$ W/m °C exhibits a different trend and suggests that $\gamma_{loc}/\gamma_{avg} = 5.5$ for $s_a/s_{max} \leq 0.80$. For $k = 5000$ W/m °C and for $s_a/s_{max} \leq 0.8$, $\gamma_{loc}/\gamma_{avg}$ equals 2.3 for the Johnson–Cook law and 3.1 for the Litonski law. For $k = 50$ W/m °C, the curve for the Litonski law shows a sharp jump in the slope at $s_a/s_{max} \approx 0.85$, indicating the rapid growth of the localization of the deformation at the specimen center. By the time the shear stress drops to 80% of its maximum value, the shear
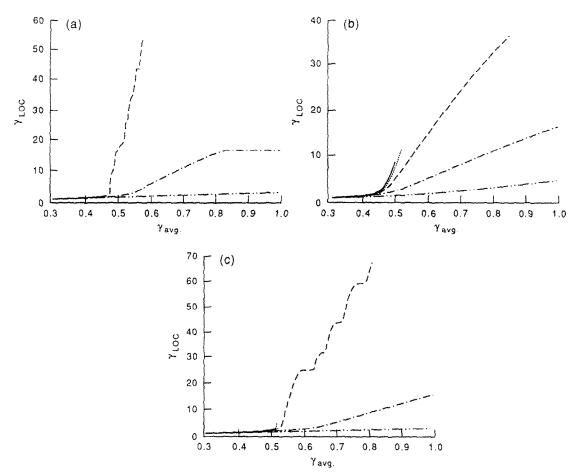
Fig. 4. Evolution of the shear strain at the specimen center for the three constitutive relations and the five values of the thermal conductivity. (a) Litonski, (b) Bodner–Partom, (c) Johnson–Cook.

strain at the specimen center would have increased enormously and the specimen would probably have failed. We recall that Marchand and Duffy [7] observed the maximum shear strain within the band to be about 20. For $k = 500$ W/m °C, $\gamma_{loc}/\gamma_{avg}$ reached a saturation value of 18 for $s_a/s_{max} \leq 0.6$ for the Bodner–Partom law. For the other two constitutive relations used, $\gamma_{loc}/\gamma_{avg}$ reached a maximum value of approximately 18 and 20 at $s_a/s_{max} \simeq 0.7$ and 0.62 for the Litonski law and the Johnson–Cook law respectively. The decrease in the value of $\gamma_{loc}/\gamma_{avg}$ signifies that the growth of the shear strain at the specimen center is less than the increase in the value of $\gamma_{avg}$. Thus the width of the severely deformed region must increase.

Marchand and Duffy [7] defined the band width as the width of the region over which the shear strain stays constant. In the problem studied herein, except when $k = 500$ or 5000 W/m °C, the band width so computed will be zero. Therefore, we define the band width as the width of the region over which the shear stain equals or exceeds 95% of its value at the specimen center. As the localization of the deformation depends upon how far the shear stress has dropped from its peak value, we have plotted in Fig. 6 the band width versus the square-root of the non-dimensional thermal conductivity $\beta$ when $s_a/s_{max} = 0.95$, 0.90, 0.85, 0.80, 0.75, and 0.70. The reason for selecting $(\beta)^{1/2}$ rather than $\beta$ as abscissa is that Dodd and Bai [43] found the band width to be proportional to $(\beta)^{1/2}$. It is clear that the dependence of the band width upon the thermal conductivity is nonlinear and is different for each of the three constitutive relations used. The band width decreases with a decrease in the value of the thermal conductivity. For the Litonski law and the Johnson–Cook law, the band width tends to zero as the thermal conductivity decreases to zero, but such is not the case for the Bodner–Partom law. For this law and for $k = 0$, the computed band width depends upon how far the shear stress at the specimen center has dropped. We note that the depicted curves were
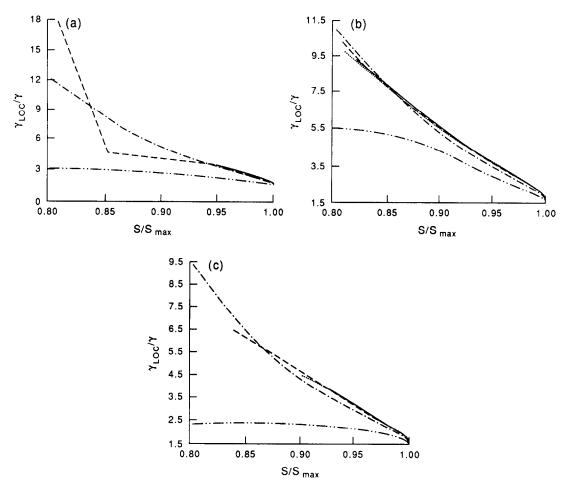
Fig. 5. Localization ratio vs $s_a/s_{max}$. (a) Litonski, (b) Bodner–Partom, (c) Johnson–Cook.

obtained by joining data points with straight lines rather than fitting a smooth curve through the data points. These curves do not support Dodd and Bai's result that the band width is proportional to $(\beta)^{1/2}$.

In Fig. 7 we have plotted the band width as a function of $s_a/s_{max}$ for the five values of the thermal conductivity and the three constitutive relations used. For $k = 50$ and $500\,W/m\,°C$, the band width does seem to reach a stable value as the shear stress at the specimen center drops. For the Litonski law, and for $k = 0$ and $5\,W/m\,°C$, satisfactory results could not be computed for $s_a/s_{max} \leq 0.95$. For the same values of $k$, and with the Johnson–Cook law, satisfactory results could not be obtained for $s_a/s_{max} \leq 0.90$. For each of the constitutive relations used, and for $k = 5000\,W/m\,°C$, an interesting situation developed in that the band width decreased first as the shear stress at the specimen center dropped. It reached a plateau at $s_a/s_{max} \approx 0.85$, and then started to increase. The rate of decrease and subsequent increase of the band width with respect to $s_a/s_{max}$ does depend upon the constitutive relation used. A plausible explanation for this computed decrease and increase of the band width is that as the shear stress at the specimen center drops and the plastic strain-rate increases sharply, the heat generated as a result of plastic working raises the temperature there more than at other points in the specimen. Initially, the rate of heat loss to outer parts of the specimen is less than the rate of heat generation at the specimen center, and the temperature there rises, making the material there softer and thus easier to deform. As the temperature gradient builds up, the rate of heat loss increases and eventually equals and exceeds the rate of heat generation at the specimen center. Thus the material surrounding the specimen center begins to deform severely, too, and the band width increases.
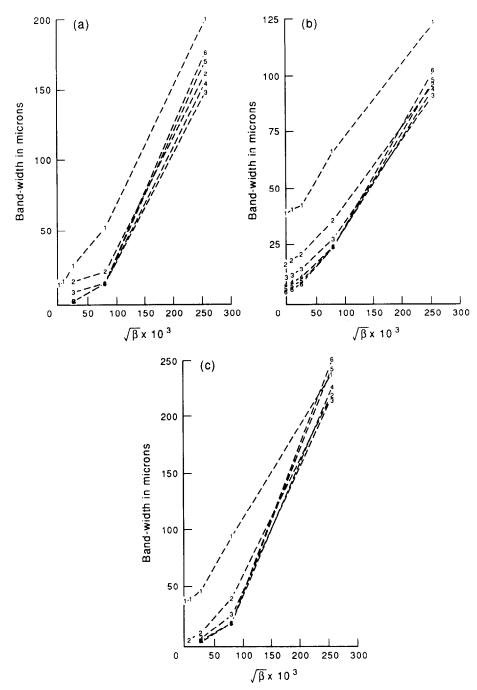
Fig. 6. Dependence of the band width upon the square-root of the non-dimensional thermal conductivity. (a) Litonski, (b) Bodner–Partom, (c) Johnson–Cook. Curve 1, $s_a/s_{max} = 0.95$; Curve 2, $s_a/s_{max} = 0.90$; Curve 3, $s_a/s_{max} = 0.85$; Curve 4, $s_a/s_{max} = 0.80$; Curve 5, $s_a/s_{max} = 0.75$; Curve 6, $s_a/s_{max} = 0.70$.

## 5. CONCLUSIONS

We have studied the problem of shear band development in a thermally softening viscoplastic block undergoing overall adiabatic deformations. The thickness of the block is assumed to vary smoothly with the thickness at the specimen center, being 5% smaller than that at the outer edges. Three constitutive relations, namely, the Litonski law, the Bodner–Partom law, and the Johnson–Cook law, have been used to represent the viscoplastic response of the material. The values of the material parameters used are such that each
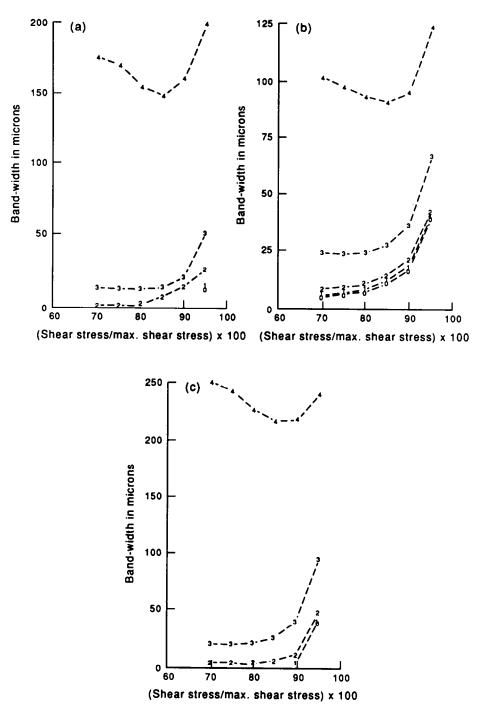
Fig. 7. Dependence of the band width upon $s_a/s_{max}$. Curve 0, $k = 0$; Curve 1, $k = 5$ W/m °C; Curve 2, $k = 50$ W/m °C; Curve 3, $k = 500$ W/m °C; Curve 4, $k = 5000$ W/m °C.

constitutive relation gives essentially the same stress–strain curve as that observed by Marchand and Duffy [7] for a HY-100 steel deformed in torsion at a strain-rate of $3300\,\mathrm{s}^{-1}$.

Results have been computed for thermal conductivity $k$ of 0, 5, 50, 500, and 5000 W/m °C. For the Bodner–Partom law, all of the results depend smoothly upon the thermal conductivity. Also, from a computational point of view, this constitutive relation was the most stable in the sense that satisfactory results could be computed for all values of $k$ considered herein.

For each of the three constitutive relations studied, the rate of evolution of the temperature at the specimen center was steepest for $k = 0$ and decreased with an increase in the value of $k$. A similar behavior was noted for the development of the shear strain at the specimen center.

When the time scale is changed to one which is proportional to $s_a/s_{max}$, the rate of temperature rise at the specimen center shows a transition for $k = 50$ W/m °C both for the Litonski law and the Johnson–Cook law. For the Litonski law and also for $k = 50$ W/m °C, the rate of localization ratio at the specimen center shows a transition at $s_a/s_{max} \approx 0.85$. Otherwise, the results depend continuously upon $s_a/s_{max}$ for the values of $k$ considered herein.

The computed band width decreases nonlinearly with a decrease in the value of $k$. Both the Litonski law and the Johnson–Cook law predict that the band width will decrease to zero as $k$ tends to zero. However, the Bodner–Partom law gives a finite value of the band width for $k = 0$. The band width was not found to be proportional to the square-root of the thermal conductivity as asserted by Dodd and Bai.

## REFERENCES

[1] A. M. MERZER, J. Mech. Phys. Solids 30, 323 (1982).
[2] F. H. WU and L. B. FREUND, J. Mech. Phys. Solids 32, 119 (1984).
[3] G. L. MOSS, In Shock Waves and High Strain Rate Phenomenon in Metals (Edited by M. A. MEYER and L. E. MURR), pp. 299–312. Plenum Press, New York, (1981).
[4] L. S. COSTIN, E. E. CRISMAN, R. H. HAWLEY and J. DUFFY, Int. Phys. Conf. Ser. 47, 90 (1979).
[5] K. A. HARTLEY, J. DUFFY and R. H. HAWLEY, J. Mech. Phys. Solids 35, 283 (1987).
[6] J. H. GIOVANOLA, Mech. Mater. 7, 59 (1988).
[7] A. MARCHAND and J. DUFFY, J. Mech. Phys. Solids 36, 251 (1988).
[8] M. R. STAKER, Acta Metall. 29, 683 (1981).
[9] R. J. CLIFTON, NRC National Material Advisory Board (U.S.) Rep. 356 (1980).
[10] R. J. CLIFTON and A. MOLINARI, J. Appl. Mech. 54, 806 (1987).
[11] T. J. BURNS, Q. Appl. Math. 43, 65 (1985).
[12] L. ANAND, K. H. KIM and T. G. SHAWKI, Massachusetts Institute of Technology Report (1986).
[13] Y. L. BAI, Shock Waves and High Strain Rate Phenomenon in Metals (Edited by M. A. MEYERS and L. E. MURR), pp. 277–283. Plenum Press, New York (1981).
[14] B. D. COLEMAN and M. L. HODGDON, Arch. Rational Mech. Anal. 90, 219 (1985).
[15] T. W. WRIGHT, J. Mech. Phys. Solids 38, 515 (1990).
[16] R. J. CLIFTON, J. DUFFY, K. S. HARTLEY and T. G. SHAWKI, Scripta Metall. 18, 443 (1984).
[17] T. W. WRIGHT and R. C. BATRA, Int. J. Plasticity 1, 205 (1985).
[18] T. W. WRIGHT and R. C. BATRA, Proc. IUTAM Symposium on Macro- and Micro-Mechanics of High Velocity Deformation and Fracture (Edited by K. KAWATA and J. SHIOIRI), pp. 189–201. Springer-Verlag, Heidelberg (1987).
[19] T. W. WRIGHT and J. W. WALTER, J. Mech. Phys. Solids 35, 701 (1987).
[20] R. C. BATRA, Int. J. Plasticity 3, 75 (1987).
[21] R. C. BATRA, Int. J. Solids Struct. 23, 1435 (1987).
[22] R. C. BATRA, J. Appl. Mech. 55, 229 (1988).
[23] C. FRESSENGEAS, Int. J. Impact Engr 8, 141 (1989).
[24] T. G. SHAWKI and R. J. CLIFTON, Mech. Mater. 8, 13 (1989).
[25] J. LEMONDS and A. NEEDLEMAN, Mech. Mater. 5, 339 (1986).
[26] J. LEMONDS and A. NEEDLEMAN, Mech. Mater. 5, 363 (1986).
[27] A. NEEDLEMAN, J. Appl. Mech. 56, 1 (1989).
[28] R. C. BATRA and D. S. LIU, J. Appl. Mech. 56, 527 (1989).
[29] R. C. BATRA and D. S. LIU, Int. J. Plasticity 6, 231 (1990).
[30] L. ANAND, A. M. LUSH and K. H. KIM, In Thermal Aspects in Manufacturing (Edited by M. H. ATTIA and L. KOPS), ASME-PED 30, 89 (1988).
[31] Z. G. ZHU and R. C. BATRA, Acta Mech. 84, 89 (1990).
[32] R. C. BATRA and X.-T. ZHANG, Acta Mech. 85, 221 (1990).
[33] R. C. BATRA and Z. G. ZHU, Int. J. Solids Struct. 27, 1829 (1991).
[34] Z. G. ZHU and R. C. BATRA, Comput. Struct. (in press).
[35] R. C. BATRA and Z. G. ZHU, Acta Mech. 86, 31 (1991).
[36] T. G. SHAWKI, R. J. CLIFTON and G. MAJDA, Tech. Rep. ARO-DAAG29-81-K-0121/3, Brown University, Providence, RI (1983).
[37] A. V. SULIJOADIKUSUMO and O. W. DILLON, Jr, J. Thermal Stresses 2, 97 (1979).
[38] W. S. FARREN and G. I. TAYLOR, Proc. R. Soc. Lond. A107, 422 (1925).
[39] S. R. BODNER and Y. PARTOM, J. Appl. Mech. 42, 385 (1975).
[40] G. R. JOHNSON and W. H. COOK, Proc. 7th Int. Symp. Ballistics, The Hague, pp. 1–7 (1983).
[41] C. W. GEAR, Numerical Initial Value Problems in Ordinary Differential Equations. Prentice-Hall, Englewood Cliffs, NJ (1971).
[42] A. C. HINDMARSH, In: Scientific Computing (Edited by R. S. STEPLEMAN et al.), pp. 55–64. North-Holland, Amsterdam (1983).
[43] B. DODD and Y. BAI, Mater. Sci. Technol. 1, 38 (1985).